Multiscale simulation of polymeric fluids using massively parallel computers

Finite Elements in Flow Problems 2017 – Rome, Italy

April 5th – 7th

Alexander Rüttgers

German Aerospace Center (DLR)

Simulation and Software Technology

Cologne, Germany

DLR

Outline

1. Modeling equations for multiscale approach
2. Numerical discretization
3. Simulation result: 3D contraction flow
4. Computational complexity

Modeling of polymeric fluids

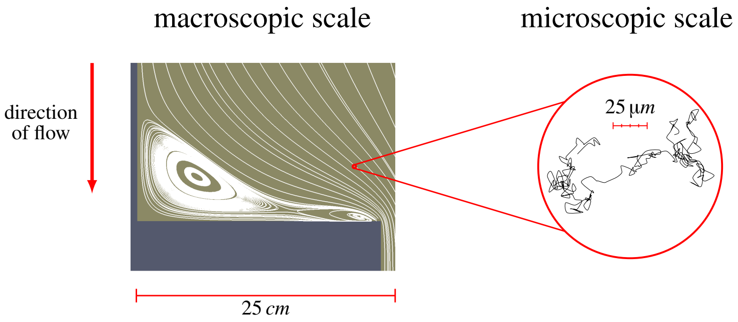

Two different modeling approaches:

overview[1]	macroscopic	multiscale
cost	low	high
modeling accuracy	low	high
drawbacks	num. instabilities	

[1] Le Bris and Lelièvre 2009

Microscale modeling

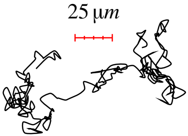

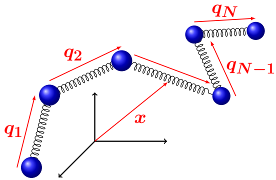

- Position vector $\boldsymbol{x}$ in flow space $\mathcal{O} \subset \mathbb{R}^3$.
- $\boldsymbol{q} = (\boldsymbol{q}_1, \ldots, \boldsymbol{q}_N)$ in configuration space $\mathcal{D} \subset \mathbb{R}^{3N}$.

MICROSCALE MODELING

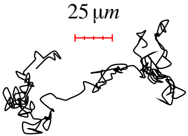

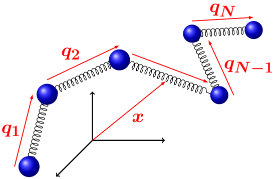

- Position vector $\boldsymbol{x}$ in flow space $\mathcal{O} \subset \mathbb{R}^3$.
- $\boldsymbol{q} = (\boldsymbol{q}_1, \ldots, \boldsymbol{q}_N)$ in configuration space $\mathcal{D} \subset \mathbb{R}^{3N}$.

Description of a polymer ensemble

- Stochastic approach:[1] random field $\boldsymbol{Q} = (\boldsymbol{Q}_1, \ldots, \boldsymbol{Q}_N)$ with $\boldsymbol{Q} : (\boldsymbol{x}, t) \in \mathcal{O} \times \mathcal{T} \mapsto \boldsymbol{Q}(\boldsymbol{x}, t)$ as $\mathcal{D}$-valued random variable.

[1] Laso and Öttinger 1993

MICROSCALE MODELING

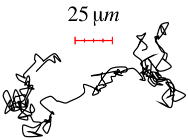

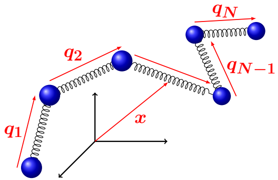

- Position vector $\boldsymbol{x}$ in flow space $\mathcal{O} \subset \mathbb{R}^3$.
- $\boldsymbol{q} = (\boldsymbol{q}_1, \ldots, \boldsymbol{q}_N)$ in configuration space $\mathcal{D} \subset \mathbb{R}^{3N}$.

Description of a polymer ensemble

- Stochastic approach:[1] random field $\boldsymbol{Q} = (\boldsymbol{Q}_1, \ldots, \boldsymbol{Q}_N)$ with $\boldsymbol{Q} : (\boldsymbol{x}, t) \in \mathcal{O} \times \mathcal{T} \mapsto \boldsymbol{Q}(\boldsymbol{x}, t)$ as $\mathcal{D}$-valued random variable.
- Fokker-Planck ansatz:[2] probability density function of field $\boldsymbol{Q}$
  - $\psi : (\boldsymbol{x}, \boldsymbol{q}, t) \in \mathcal{O} \times \mathcal{D} \times \mathcal{T} \subset \mathbb{R}^{3N+4} \mapsto \psi(\boldsymbol{x}, \boldsymbol{q}, t) \in \mathbb{R}^+$.
  - $\int_{\mathcal{D}} \psi(\boldsymbol{x}, \boldsymbol{q}, t) \, \mathrm{d}\boldsymbol{q} = 1$ for all $(\boldsymbol{x}, t) \in \mathcal{O} \times \mathcal{T}$.

[1] Laso and Öttinger 1993 , [2] Lozinski and Chauvière 2003

Coupling of micro- and macroscopic scale

- Elastic fluid behavior modeled with macroscopic stress tensor $\boldsymbol{\tau_p} : (\boldsymbol{x}, t) \in \mathcal{O} \times \mathcal{T} \mapsto \boldsymbol{\tau_p}(\boldsymbol{x}, t) \in \mathbb{R}^{3\times 3}$.

Coupling of micro- and macroscopic scale

- Elastic fluid behavior modeled with macroscopic stress tensor $\boldsymbol{\tau_p} : (\boldsymbol{x}, t) \in \mathcal{O} \times \mathcal{T} \mapsto \boldsymbol{\tau_p}(\boldsymbol{x}, t) \in \mathbb{R}^{3\times 3}$.
- **Kramers'** [1] relation for stress tensor

$$\boldsymbol{\tau_p}(\boldsymbol{x}, t) = \begin{pmatrix} \tau_{xx} & \tau_{xy} & \tau_{xz} \\ \tau_{yx} & \tau_{yy} & \tau_{yz} \\ \tau_{zx} & \tau_{zy} & \tau_{zz} \end{pmatrix} (\boldsymbol{x}, t) = C \sum_{i=1}^{N} \left(\mathbb{E}\left[\boldsymbol{Q}_i(\boldsymbol{x}, t) \otimes \boldsymbol{F}(\boldsymbol{Q}_i(\boldsymbol{x}, t)) \right] - \boldsymbol{Id} \right)$$

  - expectation $\mathbb{E}[\,\cdot\,] = \int_{\mathcal{D}} \cdot\, \psi(\boldsymbol{x}, \boldsymbol{q}, t)\, \mathrm{d}\boldsymbol{q}$ in configuration space $\mathcal{D}$.
  - spring force $\boldsymbol{F} : \mathcal{D}_i \subset \mathbb{R}^3 \to \mathbb{R}^3$.

[1] Kramers 1944

Coupling of micro- and macroscopic scale

- Elastic fluid behavior modeled with macroscopic stress tensor
  $\boldsymbol{\tau_p} : (\boldsymbol{x}, t) \in \mathcal{O} \times \mathcal{T} \mapsto \boldsymbol{\tau_p}(\boldsymbol{x}, t) \in \mathbb{R}^{3\times 3}$.

- **Kramers'** [1] relation for stress tensor

$$\boldsymbol{\tau_p}(\boldsymbol{x}, t) = \begin{pmatrix} \tau_{xx} & \tau_{xy} & \tau_{xz} \\ \tau_{yx} & \tau_{yy} & \tau_{yz} \\ \tau_{zx} & \tau_{zy} & \tau_{zz} \end{pmatrix}(\boldsymbol{x}, t) = C \sum_{i=1}^{N} \left(\mathbb{E}\left[\boldsymbol{Q}_i(\boldsymbol{x}, t) \otimes \boldsymbol{F}(\boldsymbol{Q}_i(\boldsymbol{x}, t)) \right] - \boldsymbol{Id} \right)$$

  - expectation $\mathbb{E}[\,\cdot\,] = \int_{\mathcal{D}} \cdot\, \psi(\boldsymbol{x}, \boldsymbol{q}, t)\, \mathrm{d}\boldsymbol{q}$ in configuration space $\mathcal{D}$.
  - spring force $\boldsymbol{F} : \mathcal{D}_i \subset \mathbb{R}^3 \to \mathbb{R}^3$.

- Various spring force models $\boldsymbol{F}$ in the literature
  - **Hooke** model : $\boldsymbol{F}(\boldsymbol{Q}_i) = \boldsymbol{Q}_i$ (linear)
  - **FENE** model[2] : $\boldsymbol{F}(\boldsymbol{Q}_i) = \frac{\boldsymbol{Q}_i}{1 - \|\boldsymbol{Q}_i\|^2/b}$ with $\|\boldsymbol{Q}_i\|^2 \leq b \in \mathbb{R}^+$ (nonlinear)
  - **CPAIL** model[3]: $\boldsymbol{F}(\boldsymbol{Q}_i) = \frac{1 - \|\boldsymbol{Q}_i\|^2/(3b)}{1 - \|\boldsymbol{Q}_i\|^2/b} \boldsymbol{Q}_i$ with $\|\boldsymbol{Q}_i\|^2 \leq b \in \mathbb{R}^+$ (nonlinear)

[1] Kramers 1944, [2] Warner 1972 , [3] Cohen 1991

STOCHASTIC MULTISCALE SYSTEM

$$\frac{D\boldsymbol{U}(\boldsymbol{x},t)}{Dt} = -\nabla P(\boldsymbol{x},t) + \frac{\beta}{Re}\Delta\boldsymbol{U}(\boldsymbol{x},t) + \frac{1}{Re}\nabla\cdot\boldsymbol{\tau_p}(\boldsymbol{x},t) \tag{1}$$

$$\nabla\cdot\boldsymbol{U}(\boldsymbol{x},t) = 0 \tag{2}$$

$$\begin{aligned} d\boldsymbol{Q}(\boldsymbol{x},t) = \Big[&-\boldsymbol{U}(\boldsymbol{x},t)\nabla\boldsymbol{Q}(\boldsymbol{x},t) + (\nabla\boldsymbol{U}(\boldsymbol{x},t))^T\boldsymbol{Q}(\boldsymbol{x},t) \\ &-\frac{1}{4\,De}\boldsymbol{A}\cdot\boldsymbol{F}\left(\boldsymbol{Q}(\boldsymbol{x},t)\right)\Big]\,dt + \sigma d\boldsymbol{W}(t) \end{aligned} \tag{3}$$

$$\boldsymbol{\tau_p}(\boldsymbol{x},t) = C\sum_{i=1}^{N}\left(\mathbb{E}\left[\boldsymbol{Q}_i(\boldsymbol{x},t)\otimes\boldsymbol{F}(\boldsymbol{Q}_i(\boldsymbol{x},t))\right] - \boldsymbol{Id}\right). \tag{4}$$

for the unknown random fields $\boldsymbol{U}$, P, $\boldsymbol{Q}$, $\boldsymbol{\tau_p}$,
dimensionless parameters $De, Re, \beta, \sigma \in \mathbb{R}^+$
$+$ initial and boundary conditions.

- (1)+(2) Navier-Stokes equations (macroscopic)
- (3) Stochastic PDE (microscopic)
- (4) upscaling from micro- to macroscopic scale

STOCHASTIC APPROACH FOR MICROSCALE[1,2]

- Approximation of random field $\boldsymbol{Q}(\boldsymbol{x}_k, t)$ at discrete points $\boldsymbol{x}_k$ with $3N$-dimensional **samples** $\boldsymbol{Q}^{(j)}(\boldsymbol{x}_k, t) \sim \psi(\boldsymbol{x}_k, \cdot, t)$ for $j = 1, \ldots, M_s$.

[1] Hulsen et al. 1997, [2] Laso and Öttinger 1993

STOCHASTIC APPROACH FOR MICROSCALE[1,2]

- Approximation of random field $\boldsymbol{Q}(\boldsymbol{x}_k, t)$ at discrete points $\boldsymbol{x}_k$ with $3N$-dimensional **samples** $\boldsymbol{Q}^{(j)}(\boldsymbol{x}_k, t) \sim \psi(\boldsymbol{x}_k, \cdot, t)$ for $j = 1, \ldots, M_s$.
- Monte Carlo approximation of expectation

$$
\begin{aligned}
\tau_{\boldsymbol{p}}(\boldsymbol{x}_k, t) \; &= \; C \sum_{i=1}^{N} \left(\mathbb{E}\left[\boldsymbol{Q}_i(\boldsymbol{x}_k, t) \otimes \boldsymbol{F}_i(\boldsymbol{Q}_i(\boldsymbol{x}_k, t)) \right] - \boldsymbol{Id} \right) \\
&\approx C \sum_{i=1}^{N} \left(\frac{1}{M_s} \sum_{j=1}^{M_s} \boldsymbol{Q}_i^{(j)}(\boldsymbol{x}_k, t) \otimes \boldsymbol{F}_i(\boldsymbol{Q}_i^{(j)}(\boldsymbol{x}_k, t)) - \boldsymbol{Id} \right) .
\end{aligned}
$$

[1] Hulsen et al. 1997, [2] Laso and Öttinger 1993

STOCHASTIC APPROACH FOR MICROSCALE[1,2]

- Approximation of random field $\boldsymbol{Q}(\boldsymbol{x}_k, t)$ at discrete points $\boldsymbol{x}_k$ with $3N$-dimensional **samples** $\boldsymbol{Q}^{(j)}(\boldsymbol{x}_k, t) \sim \psi(\boldsymbol{x}_k, \cdot, t)$ for $j = 1, \ldots, M_s$.
- Monte Carlo approximation of expectation

$$
\begin{aligned}
\boldsymbol{\tau_p}(\boldsymbol{x}_k, t) &= C \sum_{i=1}^{N} \Big(\mathbb{E}\big[\boldsymbol{Q}_i(\boldsymbol{x}_k, t) \otimes \boldsymbol{F}_i(\boldsymbol{Q}_i(\boldsymbol{x}_k, t))\big] - \boldsymbol{Id} \Big) \\
&\approx C \sum_{i=1}^{N} \left(\frac{1}{M_s} \sum_{j=1}^{M_s} \boldsymbol{Q}_i^{(j)}(\boldsymbol{x}_k, t) \otimes \boldsymbol{F}_i(\boldsymbol{Q}_i^{(j)}(\boldsymbol{x}_k, t)) - \boldsymbol{Id} \right).
\end{aligned}
$$

- **Variance error** in $\boldsymbol{\tau_p}$ is of order $\mathcal{O}(M_s^{-1/2})$.

---

[1] Hulsen et al. 1997, [2] Laso and Öttinger 1993

Stochastic approach for microscale[1,2]

- Approximation of random field $\boldsymbol{Q}(\boldsymbol{x}_k, t)$ at discrete points $\boldsymbol{x}_k$ with $3N$-dimensional **samples** $\boldsymbol{Q}^{(j)}(\boldsymbol{x}_k, t) \sim \psi(\boldsymbol{x}_k, \cdot, t)$ for $j = 1, \dots, M_s$.
- Monte Carlo approximation of expectation

$$\begin{aligned}\boldsymbol{\tau_p}(\boldsymbol{x}_k, t) &= C \sum_{i=1}^{N} \left(\mathbb{E}\left[\boldsymbol{Q}_i(\boldsymbol{x}_k, t) \otimes \boldsymbol{F}_i(\boldsymbol{Q}_i(\boldsymbol{x}_k, t))\right] - \boldsymbol{Id} \right) \\ &\approx C \sum_{i=1}^{N} \left(\frac{1}{M_s} \sum_{j=1}^{M_s} \boldsymbol{Q}_i^{(j)}(\boldsymbol{x}_k, t) \otimes \boldsymbol{F}_i(\boldsymbol{Q}_i^{(j)}(\boldsymbol{x}_k, t)) - \boldsymbol{Id} \right).\end{aligned}$$

- **Variance error** in $\boldsymbol{\tau_p}$ is of order $\mathcal{O}(M_s^{-1/2})$.

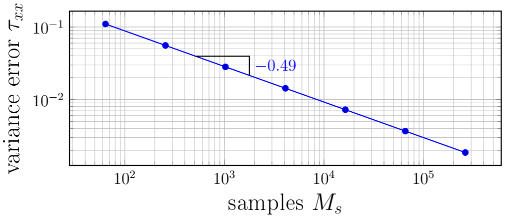

[1] Hulsen et al. 1997, [2] Laso and Öttinger 1993

Temporal evolution of microscopic scale

- Density ψ only known at $t = 0$ for complex spring models.
- At $t = 0$ create stochastic samples using **rejection sampling**[1].

temporal evolution
of stoch. samples

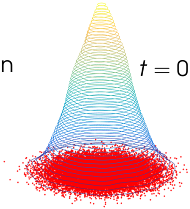

[1] von Neumann 1951

Temporal evolution of microscopic scale

- Density ψ only known at $t = 0$ for complex spring models.
- At $t = 0$ create stochastic samples using **rejection sampling**[1].
- For $t > 0$: Semi-implicit **Euler-Maruyama** scheme
  with 1. order accuracy in time.

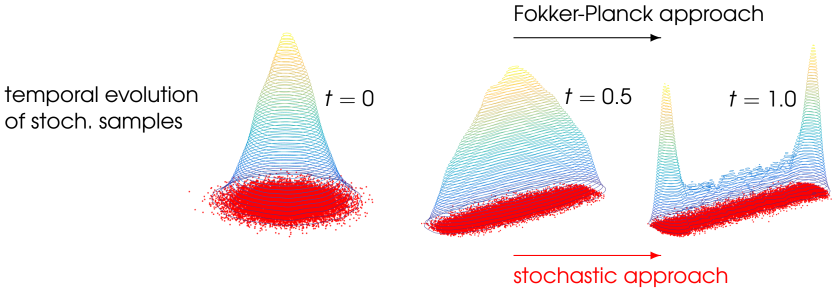

[1] von Neumann 1951

Simulation: 3D contraction flow

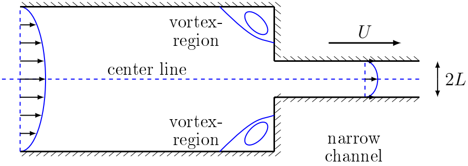

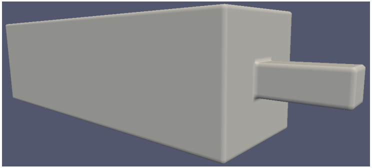

- Applications: injection moulding, polymer processing, ...
- Discretization in space with 3D flow solver *NaSt3dGPF*[1,2,3] on a staggered grid of size M_g with center $\boldsymbol{x}_k$.

[1] Griebel et al. 1998, [2] Croce et al. 2009 [3] For non-profit use: `http://wissrech.ins.uni-bonn.de`

SIMULATION: 3D CONTRACTION FLOW

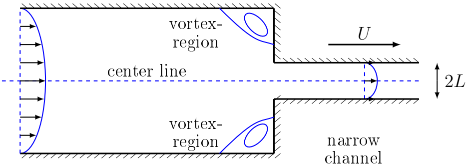

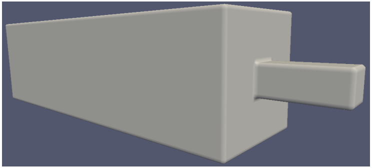

- Applications: injection moulding, polymer processing, ...
- Discretization in space with 3D flow solver *NaSt3dGPF*[1,2,3] on a staggered grid of size M_g with center $\boldsymbol{x}_k$.
- Dimensionless characteristic units:

Reynolds number: $Re = \dfrac{2L\rho U}{\eta(\dot{\gamma})}$, **Deborah number:** $De = \dfrac{\lambda U}{L}$

U average velocity, λ relaxation time,
$\eta(\dot{\gamma})$ viscosity, $\dot{\gamma}$ shear rate, L characteristic length

[1] Griebel et al. 1998, [2] Croce et al. 2009 [3] For non-profit use: `http://wissrech.ins.uni-bonn.de`

Shear-thinning fluid in $4:1$ contraction

- Experimental measurements:[1]
  - fluid: Glycerol $+$ water $+$ PAA (600ppm)
  - relaxation time: $\lambda = 32s$
  - experimental Deborah numbers: $De = 1, \ldots, 200$

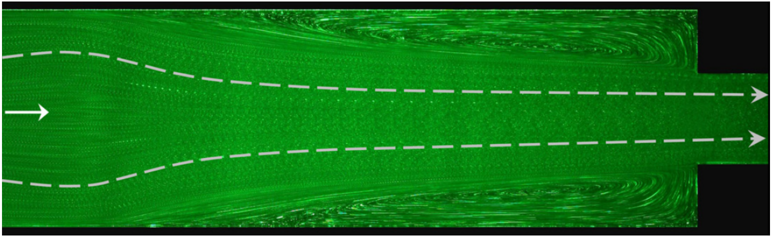

FIGURE: Visualization of contraction flow[1] with $Re = 2.37$, $De = 174$

[1] Sousa, Coelho, Oliveira and Alves 2011

Shear-thinning fluid in 4 : 1 contraction

- Experimental measurements:[1]
  - fluid: Glycerol + water + PAA (600ppm)
  - relaxation time: $\lambda = 32\mathrm{s}$
  - experimental Deborah numbers: $De = 1, \ldots, 200$
- For high Deborah number flows:
  - large corner vortices occur
  - streamline divergence
  - inverted streamline rotation
- Macroscopic approaches often suffer from numerical instabilities[2,3].

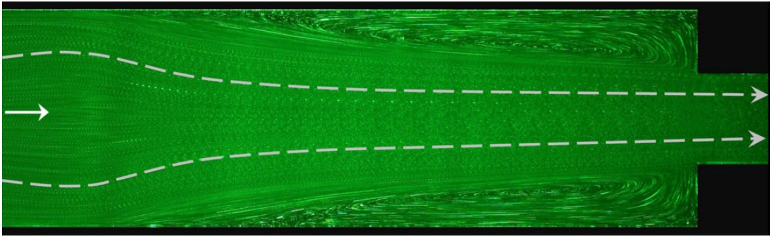

FIGURE: Visualization of contraction flow[1] with $Re = 2.37,\ De = 174$

[1] Sousa, Coelho, Oliveira and Alves 2011, [2] Keunings 1986 , [3] Mangoubi et al. 2009

3D SIMULATION RESULTS[1]

- 8 multiscale simulations.

Simulation parameters	
Deborah number De	24.1, 108, 157
spring model	FENE chain
spring segments N	1, 3, 5
resolution M_g	$380 \times 64 \times 64$
samples per cell M_s	1200

[1] partial results in Griebel and R. 2014

3D SIMULATION RESULTS[1]

- 8 multiscale simulations.
- All elastic effects reproduced in simulation.
- No stability issues occurred.

Simulation parameters	
Deborah number De	24.1, 108, 157
spring model	FENE chain
spring segments N	$1, 3, 5$
resolution M_g	$380 \times 64 \times 64$
samples per cell M_s	1200

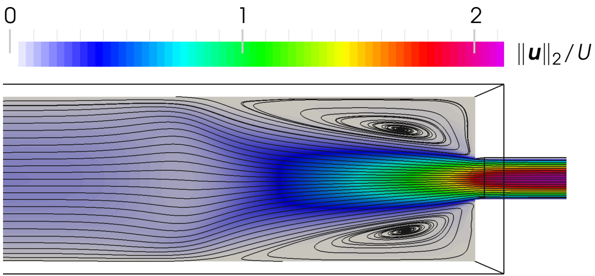

FIGURE: Simulation of 5-segment chain with $De = 157$.

[1] partial results in Griebel and R. 2014

3D SIMULATION RESULTS[1]

- 8 multiscale simulations.
- All elastic effects reproduced in simulation.
- No stability issues occurred.

Simulation parameters	
Deborah number De	24.1, 108, 157
spring model	FENE chain
spring segments N	1, 3, 5
resolution M_g	$380 \times 64 \times 64$
samples per cell M_s	1200

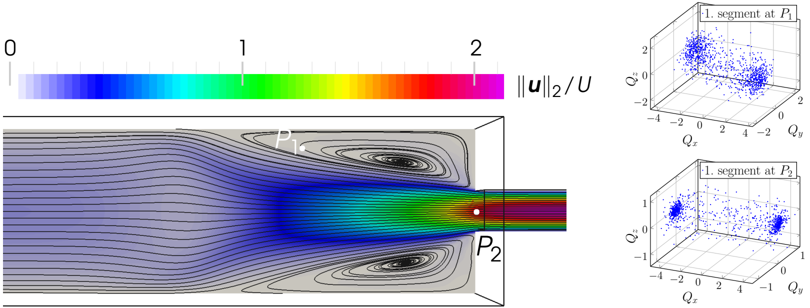

FIGURE: Simulation of 5-segment chain with $De = 157$.

[1] partial results in Griebel and R. 2014

Comparison of experiment and simulation

- Velocity profiles compared on the channel's centerline (a).
- Inverted 3D streamline rotation compared to Newtonian flow (b+c).
- Simulation results correspond with experimental measurements.

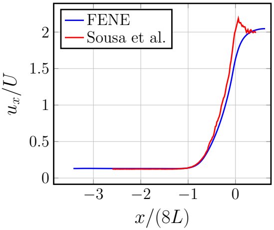

(a) velocity profile $De = 24$

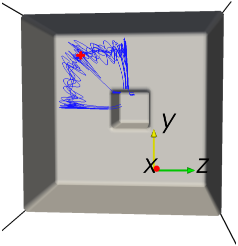

(b) streamlines $De = 1.0$

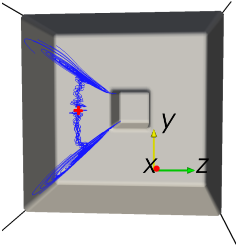

(c) streamlines $De = 157$

COMPLEXITY OF MULTISCALE SIMULATIONS

Clusters for multiscale simulations

	Atacama	**JUROPA**
# cores	1,248 CPUs	17,664 CPUs
memory	4,992 GB	52,992 GB
Linpack	$\approx$21 TFlops/s	207 TFlops/s
installation	Mar 2014	access: 11/2013 - 10/2014

Institute for Numerical Simulation, University of Bonn
Jülich Supercomputing Centre, Jülich Research Centre

(a) INS cluster

(b) Juropa racks

Complexity of multiscale simulations

- M_g grid cells in space,
- M_s samples per grid cell,
- spring model with N segments.

Complexity of multiscale simulations

- M_g grid cells in space,
- M_s samples per grid cell,
- spring model with N segments.

Complexity of stochastic microscale	
spatial grid M_g	$380 \times 64 \times 64$
samples per cell M_s	1200
total samples	$1.87 \cdot 10^9$
spring segments N	5
sample dimensionality	15-dim
storage	**208 GB**
computing time (256 CPUs)	7-8 weeks

Complexity of multiscale simulations

- M_g grid cells in space,
- M_s samples per grid cell,
- spring model with N segments.

Complexity of stochastic microscale	
spatial grid M_g	$380 \times 64 \times 64$
samples per cell M_s	1200
total samples	$1.87 \cdot 10^9$
spring segments N	5
sample dimensionality	15-dim
storage	**208 GB**
computing time (256 CPUs)	7-8 weeks

Solution approach

1. Parallelization
2. Model reduction:
   - proper generalized decompositon (PGD)[1]
   - sparse grids[2]

[1] Chinesta, Ammar, Leygue and Keunings 2011, [2] Delaunay, Lozinski and Owens 2007

Sparse grid combination technique[1]

- Approximation of full grid solution $\boldsymbol{u_l} \in V_{\boldsymbol{l}}$ as a **combination of coarse full grid solution spaces $\boldsymbol{u_m} \in V_{\boldsymbol{m}}$.**
- Multi-indices $\boldsymbol{m}, \boldsymbol{l} \in \mathbb{N}^d$ denote discretization accuracy.

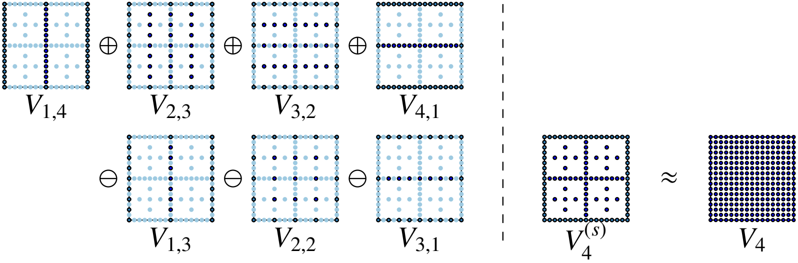

FIGURE: Combination technique (left), sparse grid (center) and full grid (right).

[1] Griebel, Schneider, Zenger 1992, [2] R. and Griebel, submitted to Appl Math & Comput

Sparse grid combination technique[1]

- Approximation of full grid solution $\boldsymbol{u_l} \in V_{\boldsymbol{l}}$ as a **combination of coarse full grid solution spaces $\boldsymbol{u_m} \in V_{\boldsymbol{m}}$**.
- Multi-indices $\boldsymbol{m}, \boldsymbol{l} \in \mathbb{N}^d$ denote discretization accuracy.
- Combination technique is **intrinsically parallel**.
- Existing multiscale solver can be **reused**.
- **Numerical result:** Computational effort **reduced by one order of magnitude** in shear and extensional flows[2].

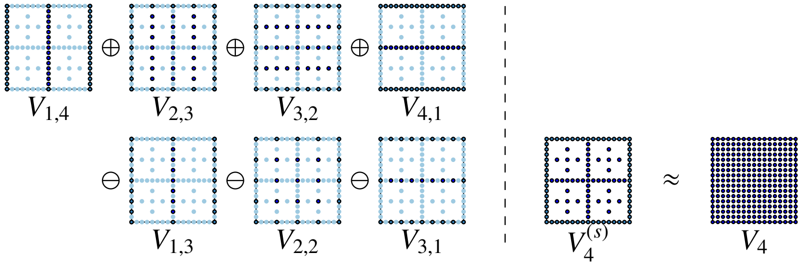

FIGURE: Combination technique (left), sparse grid (center) and full grid (right).

[1] Griebel, Schneider, Zenger 1992, [2] R. and Griebel, submitted to Appl Math & Comput

Summary

1. Simulation of 3D contraction flow with multiscale model:
   - Results compared with experimental measurements from the literature.
   - Experimental phenomena could be reproduced.

Summary

1. Simulation of 3D contraction flow with multiscale model:
   - Results compared with experimental measurements from the literature.
   - Experimental phenomena could be reproduced.
2. Reduction of enormous computing time with (twofold parallelism)
   - parallelization (*Atacama* 1248 CPUs).
   - sparse grid combination technique.

Summary

1. Simulation of 3D contraction flow with multiscale model:
   - Results compared with experimental measurements from the literature.
   - Experimental phenomena could be reproduced.
2. Reduction of enormous computing time with (twofold parallelism)
   - parallelization (*Atacama* 1248 CPUs).
   - sparse grid combination technique.

Thank you for your attention!

References (1/3)

1. C. Le Bris, T. Lelièvre.
   Multiscale modelling of complex fluids: a mathematical initiation
   Multiscale Modeling and Simulation in Science, 49–137, 2009
2. M. Laso, H. Öttinger.
   Calculation of viscoelastic flow using molecular models
   J Non-Newton Fluid Mech, 47:1–20, 1993
3. A. Lozinski, C. Chauvière.
   A fast solver for Fokker–Planck equation applied to viscoelastic flows calculations
   J Comp Phys, 189:607–625, 2003
4. H. Warner.
   Kinetic theory and rheology of dilute suspensions of finitely extendible dumbbells
   Ind Eng Chem Fundam, 11:379–387, 1972
5. A. Cohen.
   A Padé approximant to the inverse Langevin function
   Rheologica Acta, 30:270–273, 1991
6. A. Chorin
   Numerical solution of the Navier-Stokes equations
   Math. of Comput., 22:745–762, 1968
7. M. Hulsen, A. Van Heel, B. Van Den Brule
   Simulation of viscoelastic flows using Brownian configuration fields
   J Non-Newton Fluid Mech, 70:79–101, 1997

REFERENCES (2/3)

8. J. von Neumann
   Various techniques used in connection with random digits. Monte Carlo methods
   Nat Bur Stand, 12:36–38, 1951
9. M. Griebel, T. Dornseifer, T. Neunhoeffer
   Numerical Simulation in Fluid Dynamics, a Practical Introduction
   SIAM, Philadelphia, 1998
10. R. Croce, M. Griebel, M.A. Schweitzer
    Numerical simulation of bubble and droplet-deformation by a level set approach with surface tension in three dimensions
    Int J Numer Methods Fluids, 62:963–993, 2009
11. P. Sousa, P. Celho, M. Oliveira, M. Alves
    Effect of the contraction ratio upon viscoelastic fluid flow in three-dimensional square–square contractions
    Chem Eng Sci, 66:998–1009, 2011
12. R. Keunings **On the high Weissenberg number problem**
    J Non-Newton Fluid Mech, 20:209–226, 1986
13. C. Mangoubi, M. Hulsen, R. Kupferman
    Numerical stability of the method of Brownian configuration fields
    J Non-Newton Fluid Mech, 157:188–196, 2009
14. M. Griebel, A. Rüttgers
    Multiscale simulations of 3D viscoelastic flows in a square-square contraction
    J Non-Newton Fluid Mech, 205:41-63, 2014

References (3/3)

15. F. Chinesta, A. Ammar, A. Leygue, R. Keunings
An overview of the proper generalized decomposition with applications in computational rheology
J Non-Newton Fluid Mech, 166:578–592, 2011
16. P. Delaunay, A. Lozinski, R. Owens
Sparse tensor-product Fokker-Planck-based methods for nonlinear bead-spring chain models of dilute polymer solutions
CRM Proc, 41:73–89, 2007
17. M. Griebel, M. Schneider, C. Zenger
A combination technique for the solution of sparse grid problems
Iterative Meth Lin Alg, 263–281, 1992
18. A. Rüttgers, M. Griebel
Multiscale simulation of polymeric fluids using the sparse grid combination technique
submitted to *Appl Math & Comput*